A Novel Metric to Quantify and Enable Resilient Distribution System Using Graph Theory and Choquet Integral

Prabodh Bajpai, *Senior Member, IEEE*, Sayonsom Chanda, *Member, IEEE*, and Anurag K. Srivastava, *Senior Member, IEEE*

***Abstract*—Network operators and utilities are challenged with increasing extreme weather conditions, resulting in interrupted power supply to critical loads. Resiliency metrics, which can capture the level of preparedness to resist adverse impact of extreme conditions on a distribution system, can be leveraged in multiple ways to provide better operation of the network and design of the future systems. In this paper, a methodology to quantify resiliency and maintain power supply to critical loads (CLs) during extreme contingencies has been proposed. Resiliency evaluation of power distribution system has been defined as a multi-criteria decision making problem and quantified using graph theoretic approach and Choquet integral. The algorithm proposed in this paper to calculate the resiliency for all feasible network configurations supplying CLs in a network is useful in planning as well as operation of the distribution network. The application of the proposed algorithm is demonstrated through several case studies using two proximal CERTS microgrids and IEEE 123 node distribution system. Simulation studies are also provided for planning of resilient network, by placing additional switches in the considered distribution systems with microgrid.**

***Index Terms*—Choquet integrals, distribution system, graph theory, multiple microgrids, reconfiguration, resiliency.**

I. Introduction

POWER outages lead to financial loss of an average of $80 billion annually in the United States. These outages result from a variety of factors, such as weather [1], inadequate generation, and transmission failure [2]. The increase in number of extreme weather events (e.g., Hurricane Sandy in 2012) coincident with the increasing demand of reliable power mainly resulted in greater emphasis on resiliency of power distribution system (PDS) [3].

During extreme weather events, resiliency efforts should focus on rectifying service interruptions to critical loads (CLs), such as airports, hospitals, city halls, and the other buildings deemed important to the community as providing power to all the connected loads during extreme events will be economically infeasible [4], [5].

In anticipation of more power interruptions due to weather and progressive climate change, there has been an increased community-wide emphasis on "developing more resilient critical infrastructure", which is essential to the security and prosperity of the community [6]. Traditional methods of measuring PDS efficiency and reliability might be inadequate to address resiliency. There are several working definitions of resiliency, according to [7]–[9], which can be summarized as "Resilience includes the ability to withstand and recover from deliberate attacks, accidents, or naturally occurring threats or incidents."

Some researchers have proposed formulating resiliency metrics considering the entire infrastructure of a community or a city [9]. Their method comprises survey of all the resources available to the entire community for their index. However, their method is not focused on PDS, and thus cannot be effectively used for electrical engineering purposes. There are several methods of determining resilience of energy infrastructure as proposed by [8] and [10]–[12]. Kwasinski [13] have provided framework to measure and assess the resilience of a PDS emphasizing on customer benefits. However, such models are probabilistic, and computation of the probability of an event occurring depends on several other factors and are prone to errors.

Evaluation of PDS resiliency will improve the control decisions taken by a distribution network operator (DNO) as a corrective or precautionary measures. Additionally, it would make it easier to channelize funds and efforts towards making the power grid better in the long term. The proposed method can be used to incorporate recent advancements in distribution automation [14], and applications of technologies such as optimal scheduling model to improve resiliency of microgrid-based power distribution system [15] .

Mostly, resiliency studies of critical infrastructure have used complex network theory. The application of complex network theory to evaluate resilience of physical complex networked

Manuscript received February 15, 2016; revised June 2, 2016 and September 11, 2016; accepted October 19, 2016. Date of publication November 1, 2016; date of current version June 19, 2018. This work was supported by the Indo-U.S. BASE Fellowship Program. Paper no. TSG-00212-2016.

P. Bajpai was with Washington State University, Pullman, WA 99164-1009 USA. He is now with the Department of Electrical Engineering, Indian Institute of Technology at Kharagpur, Kharagpur 721302, India.

S. Chanda was with the School of Electrical Engineering and Computer Science, Washington State University, Pullman, WA 99164-1009 USA. He is now with Idaho National Laboratory, Idaho Falls, ID 83415 USA.

A. K. Srivastava is with the School of Electrical Engineering and Computer Science, Washington State University, Pullman, WA 99164-1009 USA (e-mail: asrivast@eecs.wsu.edu).

Color versions of one or more of the figures in this paper are available online at http://ieeexplore.ieee.org.

Digital Object Identifier 10.1109/TSG.2016.2623818

infrastructures was proposed in [16] and [17]. Resilience of water distribution systems has been formulated using a complex network approach in [18]. In areas of power systems, the work presented in [19] identifies critical nodes in power system network vulnerabilities in a transmission networks.

A method has been proposed to quantify the topological resiliency of a distribution system using analytical hierarchical process (AHP) [20]. The resiliency of the power distribution network is formulated in [21] as a multi-criteria decision making problem. In [22], a two-stage stochastic model to support decision making process for power system restoration in pre-hurricane phase is introduced using Benders' decomposition. In [23], preventive reinforcement strategies are offered to the microgrid operators to improve the resiliency of generation and demand scheduling against disruptions in multiple energy carrier microgrids. Microgrids have been investigated as resources for restoring critical loads in active distribution systems in [24], due to the impact of hurricanes or other natural forces.

Optimum autonomous communication requirements in microgrids has been investigated in [25] to enable resilience in PDS, after major faults in a distribution system due to natural disasters. It has been noted in review of smart grid technologies being currently employed to improve resilience of PDS that utilities rely heavily on 'experience' to take restorative actions for hardening and enabling resiliency in their systems [26]. However, formal quantification of such approaches are not yet formalized; thus, such actions are not accurate all the time, and cannot be leveraged by distribution automation systems. However, such studies have limited practicality in the near future as it would depend on logistic arrangements between multiple utilities and economic factors.

The comparative effectiveness of different network configurations in terms of their resiliency during planning and contingent operations of power distribution systems has not been considered in any of the related published work. Additionally, the number of factors impacting resiliency considered in the existing work are limited and not very comprehensive. Moreover, the physical constraints (power flow voltage limits, generation limits, thermal limits) of a PDS provide additional challenges. Resilience of a PDS is also affected by the control decisions taken by the operator or the reconfiguration method during an ongoing contingency.

Since practicality of enabling resilience in current infrastructure is a key issue, resiliency metric also needs to be translated into operator-comprehensible decision-making guidelines during the contingencies. Thus, the overall objective of the paper is to help operators in resiliency evaluation and metrics based decision making to maximize the resiliency of PDS. Contribution of this paper is the development of the resiliency metrics to quantify the resiliency based on the network topology, number of common paths to restore a load, and probability of availability of power resources to supply these loads after an adverse event. Further an approach for enabling resiliency of a given distribution network is developed using graph theory and Choquet integral. Simulation results for planning and operational case studies have been presented to validate the developed algorithms.

II. Key Factors to Impact Resiliency of PDS

Resiliency of a power system depends on the ability of system to maintain continuous supply to CLs, in events of 'low frequency, high impact' contingencies. There can be multiple ways to enable resiliency in PDS, such as storm-hardening of infrastructure, improved cyber-security and implementation of more intelligent control algorithms. Along with a combination of these factors, improved management of system redundancy will be critical to improve the resiliency of a PDS. The resiliency metric proposed in this work is based on the premise that all contributing factors to enhance resiliency will be strongly correlated to the factors described below. For the following definitions, generic PDS is considered as a graph with n nodes and e branches.

1) Branch Count Effect (BCE): This is represented by the ratio of the total number of connected branches for each path combination without loop (PCWL) in a possible network (PN) to the number of all CLs. For each PN, the average value of all corresponding similar PNs is considered.

$$\mathrm{BCE}_q = \frac{\sum_{k=1}^{N_q} \frac{\text{Nodes in PCWL for kth PN}}{\text{Number of CLs in kth PN}}}{N_q} \tag{1}$$

where, q is the q^{th} FN being considered, and N_q is the total number of similar PNs for the q^{th} FN.

2) Overlapping Branches (OB): It is defined as total number of common branches in each PCWL in a PN. Again the average value of all similar PN is considered for the corresponding FN.

$$\mathrm{OB}_q = \frac{\sum_{k=1}^{N_q} \text{Common Branches in kth PN}}{N_q}. \tag{2}$$

3) Switching Operations (SO): It is defined as the total number of changes in state of the switches, i.e., from normally closed (NC) to open and from normally open (NO) to closed, to create different FNs without any loop and connecting all CLs to a source.

4) Repetition of Sources (RoS): It refers to the ratio of the number of available sources used to supply all CLs to the number of all CLs in each PN. The average value of all similar PNs is considered for the corresponding FN. This factor should have high value for high resiliency.

$$\mathrm{RoS}_q = \frac{\sum_{k=1}^{N_q} \frac{\text{Sources supplying all CLs in kth PN}}{\text{Number of CLs in kth PN}}}{N_q}. \tag{3}$$

5) Path Redundancy (PR): This is the ratio of total number of paths available for all CLs connecting to all sources to the total number of CLs in each FN.

$$PR_q = \frac{\text{Paths connecting all CLs to all sources in qth FN}}{\text{Number of CLs in qth FN}}. \tag{4}$$

6) Probability of Availability and Penalty Factor (PoA & PF): This factor has two components to distinguish the source feeding power to the CL. One is based on reliability or probability of availability of the source, and the other is based on the losses in distribution or penalty factor. If the CL is drawing power from the main grid, the probability of availability

and penalty factor should be highest because main grid will be more reliable compared to DGs. However, reliability of all DGs to supply a CL may be assumed same but a high penalty should be considered, if power is drawn from a DG located in other MG than from a DG located in same MG, where CL is located. PoA and PF for a FN is determined by Eq. 5

$$POA\&PF_q = \frac{\sum_{k=1}^{N_q} POA \times PF \text{for kth PN}}{N_q}. \tag{5}$$

7) Aggregated Central Point Dominance (ACPD): This network metric captures the information about the importance of the node for the given topology of the network. To determine this value, central point dominance (or betweenness centrality) of each node in a path is determined using Eq. 6 to identify the importance of each node for the connectivity of the network.

$$C_B(d) = \sum_{j \neq d \neq i} \frac{\sigma_{ji}(d)}{\sigma_{ji}} \tag{6}$$

where, σ_{ji} is the total number of shortest paths from node j to i, and $\sigma_{ji}(d)$ is the number of those paths that pass through node d. To get the representation of the full network, the aggregated central point dominance of any network is defined using Eq. 7:

$$ACPD_q = \frac{\sum_{d=1}^{D} \Omega_d^q \times C_B(d)}{D_q} \tag{7}$$

where, Ω_d^q is the order of node d in the q^{th} network, and D_q is the total number of nodes in the network.

Computing the resiliency of a network is essentially mathematical modeling of interaction and simultaneous effect of several factors of resiliency metrics, which can be computationally expensive for medium to large distribution networks. Finding the number of simple paths between any two nodes is NP-hard problem [27]. For a PDS, finding the number of paths becomes even more complicated as additional switches (with normally open status) can be installed in each section, adding to the number of possible paths. They require $\mathcal{O}(n+e)$ space and run in $\mathcal{O}(ne+s)$ and $\mathcal{O}(2^s.ne+\log n)$ time to compute on unweighted and weighted networks, respectively, where $\mathcal{O}$ is a Landau notation [28], used to denote the increase in growth rate of the function when number of nodes increase, s is the number of switching states possible in the sections of the distribution system feeder(s). Since for distribution system weighted graphs will be more applicable to use, the computation time is even larger for a real PDS [29]. Hence, it is a complex problem, and one of the bottlenecks while attempting to quickly quantify the resiliency of a PDS. Several path finding algorithms (depth-first search, breadth-first search, Tarjan's Algorithm [30]) have been proposed to effectively determine the number of simple paths (i.e., a subgraph without repetition of vertices) between two nodes in a graph. There are many ways of searching a graph, depending upon the way in which branch to search are selected. When selecting a branch to traverse, always choose an edge emanating from the vertex most recently reached which still has unexplored edges. A search which uses this rule is called a depth-first search. After finding all possible paths, their different combinations lead to PNs based on operational feasibility.

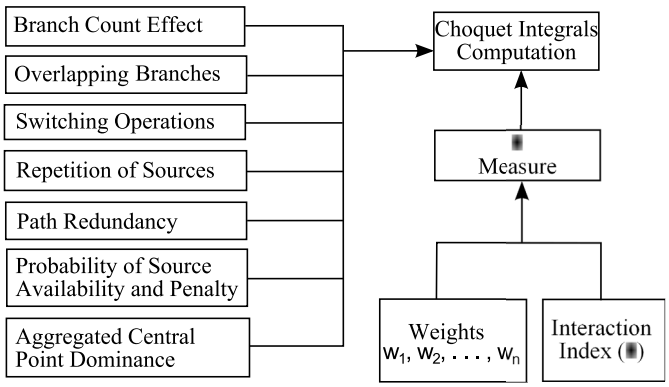

Fig. 1. Overview of resiliency quantification process.

The operational feasibility of PNs needs to be ensured by ensuring power flow constraints, IEEE standards, safety codes, and local jurisdiction specifications are adhered to.

The criteria discussed in this section are interdependent and have interactive characteristics, which cannot be evaluated by additive measures. Thus, non-additive tools of aggregating measures of different criteria deem as better tools. Therefore resiliency quantification problem of a PDS has been framed as multi-criteria decision making (MCDM) problem. Use of MCDM helps to account for all these different types of attributes without any homogeneity or a normalization requirement which speeds up the computation process [31].

III. A Metric for Quantifying Resiliency of PDS

Since unique numerical solutions are preferred for easier interpretation, Choquet Integral (CI) is a feasible approach to quantify resiliency based on several criteria [32]. Process of resiliency quantification using CI is briefly summarized in Fig. 1, where seven network metrics values are used as input and parameters of the model are input weights and interaction index.

CI is an aggregation operator which can be applied to different criteria which cannot adequately provide an answer to the problem, when considered one at a time. It uses the concept of measure and is able to account multiple interdependent criteria. There are various aggregation methods like Weighted Arithmetic Mean, Maximum and Minimum etc., but the CI provides greater flexibility. The use of CI in multi-criteria decision making has been proposed by many authors for several complex MCDM problems [32], and thus has been chosen as the method for evaluating resiliency of all FNs to supply CLs in a PDS.

The CI is based on the measure and is used for aggregation of partial values. The concept of measure in CI acts as indices on parameters which help to interpret the importance of each criterion. Measure μ_i indicates the importance of individual criteria x_i, and combinations of criteria taken together in a Set. A criteria x_i is important if value of μ_i is high. However for the importance of x_i, it may not be enough to look at only the value of μ_i but also we have to consider the value of μ_{ij}, μ_{ijk} etc. where j,k are other criteria. Now if μ_i and μ_j are high but μ_{ij} do not have much difference from μ_i and μ_j then

we can interpret that the importance of criteria x_i and x_j taken separately is same as x_i and x_j taken together. So we should not have much interest in considering them both. On the other hand if μ_i and μ_ja have low values but μ_{ij} is very large then x_i and x_j are not as much important as when both taken together.

CI is defined by several different definitions [32]: A measure μ on a set of criteria X is a function $\mu(X) \rightarrow [0, 1]$, satisfying the axioms (i) $\mu(\phi) = 0$, where ϕ represents an empty set, and (ii) $A \subset B \subset X$ implies $\mu(A) \leq \mu(B)$, A and B are non-empty sets representing different alternatives. In another definition, if measure μ on a set of criteria $X = [x_1, x_2, \ldots, x_n]$, then the CI of a function $f : X \rightarrow \mathbb{R}+$ with respect to μ is defined by Eq. 8:

$$C_\mu(f) = \int f d\mu = \sum_{i=1}^{n} (f(x_i) - f(x_{i-1}))\mu\left(A_{(i)}\right) \tag{8}$$

such that $0 \leq f(x(1)) \leq f(x(2)) \cdots \leq f(x(n))$, $A_{(i)} \in X$ and $f(x(0)) = 0$.

Eq. 8 is used to aggregate the impact of different criteria to compute the resiliency metric. The proposed resiliency quantification process considers X as a set of the seven criteria mentioned in Section II. In power networks, the criteria to determine resiliency are not independent of each other, and f determined from one criteria may impact the values from other criteria. For example, let us assume that there are two criteria 'A' and 'B' and two FN alternatives, N_1 and N_2. Also, let us assume that both the criteria, 'A' and 'B', are equally important to evaluate the resiliency with other possible criterion: $\mu(A) = \mu(B) = 0.25$. If for network N_1, criteria 'A' and 'B' complement each other to increase the resiliency, there would be a 'positive synergy' between the interacting factors, and $\mu_{N_1}(A, B) = 0.661 > \mu_{N_1}(A) + \mu_{N_1}(B) = 0.5$. On the contrary, if for network N_2, criteria 'A' and 'B' contradict each other to decrease the resiliency, there would be a 'negative synergy' between the interacting factors, and $\mu_{N_2}(A, B) = 0.425 < \mu_{N_2}(A) + \mu_{N_2}(B) = 0.5$. In the CI approach taken in this paper, a positive effect or a negative effect of a criteria on resiliency has been determined separately using weights. Thus, μ had to be determined for each network alternative. In order to identify the impact of each criteria on the overall resiliency, interaction between each criteria needs to be determined for the network. Weights assigned to these criteria are user-defined, and may be directly assigned based on computation of the resiliency factors described in Section II, and assigned by pairwise comparison for final computation of Eq. 8. For pairwise comparison, each of the criteria are taken in the order of one-at-a-time, two-at-a-time, ... seven-at-a-time to determine the measure. The weights are assigned in a typical AHP matrix to determine the overall interaction of resiliency-determining factors. If a positive synergy exists between two interacting parameters, positive weights $\in (0, 9]$ are assigned, and negative weights are assigned for negative synergy interactions.

The criteria being considered are inter-dependent and to model it, a special measure λ (called the 'interaction index' in certain literature [33]) is defined on 2^X of the finite set of criteria X, and satisfies the following criteria

$$\mu_\lambda(A \cup B) = \mu_\lambda(A) + \mu_\lambda(B) + \lambda\mu_\lambda(A)\mu_\lambda(B) \tag{9}$$

whenever $A \cap B = \phi$ and $\lambda \in (-1, \infty)$. Since X is a finite set, the λ -measure of $\mu_\lambda(X)$ can be written as [34]

$$\mu_\lambda(X) = \sum_{i}^{n} \mu_i + J \tag{10}$$

$$\text{where } J = \lambda \sum_{i_1=1}^{n-1} \sum_{i_2=1+i_1}^{n} \mu_{i_1}.\mu_{i_2} + \cdots + \lambda^{n-1}\mu_{i_1}.\mu_{i_2} \ldots \mu_{i_n}$$

$$\mu_\lambda(X) = \frac{1}{\lambda}\left[\prod_{i=1}^{n}(1 + \lambda\mu_i) - 1\right] \text{by definition, } \mu_\lambda(X) = 1$$

$$\lambda + 1 = \prod_{i=1}^{n}(1 + \lambda\mu_i) \tag{11}$$

Using Eq. 11, the interaction index is determined. After the measure for all the criteria combination is computed, using Eq. 8, all the FNs can be ranked in the order of their resiliency values.

IV. Enabling Resilient PDS

In Section II, six criteria that affect operational resiliency of the microgrid have been identified, depending on the following three axioms:

- Resiliency of a network depends on number of paths that connect a source node to a sink node.
- Increasing ratio of number of sources to number of critical load increases resiliency of the network.
- Increasing number of switches increases resiliency, but increasing number of switching operations to connect the source to sink decrease the resiliency - as more switches means more chances of them being non-functional during an emergency.

These three axioms translate into three objectives, which need to be implemented in order to enable a resilient PDS. The algorithm proposed in Fig. 2 emphasizes restoration of critical loads (loads assigned high priority) prior to restoring loads in the network. We try to restore the critical loads in a PDS by minimizing the number of switching operation requirements. Since the goal of a resilient power distribution system is to minimize any downtime, the novel approach proposed in the paper, proactively determines alternative paths and their corresponding resiliency values when a load needs to connected to source using a path that is not its regular path. It is well-understood and agreed upon (by virtue of a large number of restoration algorithm papers in literature) that a load can be restored using multiple paths. However, the approach suggested in this paper would enable an operator to take the most resilient decision. It is not easy to take decisions during contingency, and not all power system state-estimating sensors may be working correctly in a post-emergency environment. Thus, the method proposed in this paper prepares a list of paths an operator can choose, if an emergency occurs. Switching operation to restore critical loads by the operator is mathematically guaranteed to have least probability of further failures in the system.

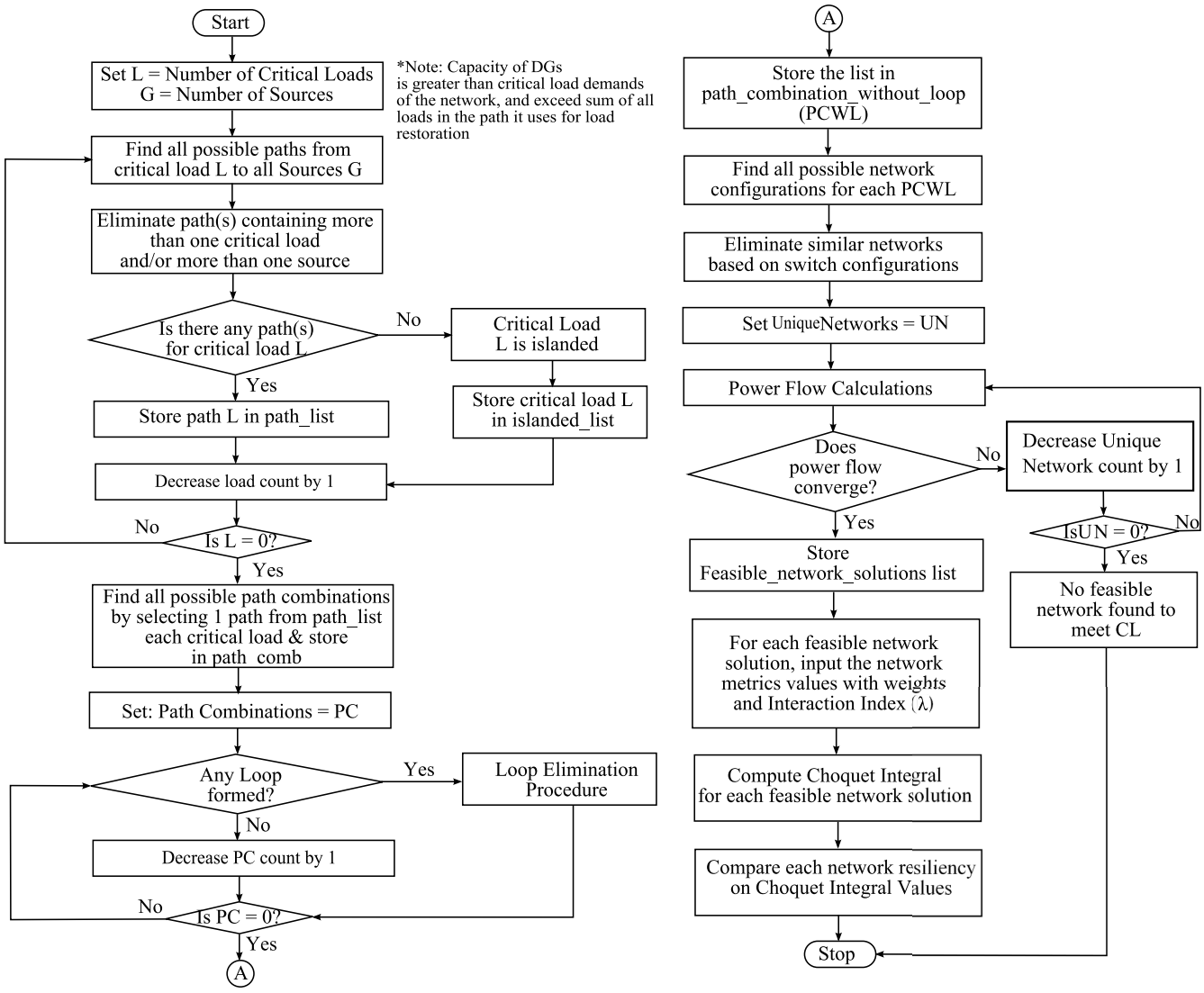

Fig. 2. Algorithm for enabling resiliency through PN soultions and their resiliency quantification.

To determine the operationally FN solutions to meet all CLs during planning and operational contingency, it is important to start by determining the CLs and sources available in the network. Then find all possible path combinations taking one path for each CL. To maintain the radial nature of the PDS path combinations with loop are eliminated using loop elimination technique [35].

The reconfiguration problem of multiple microgrids discussed in this paper has three objectives, which are to maximize the number of the energized loads, to minimize the number of switching, and to maximize the utilization of power under different contingent conditions. The algorithm for enabling resiliency through PN solutions and their resiliency quantification is shown in Fig. 2. It is also worth noting that the resiliency indices determined from Fig. 2 are functions of operating conditions at a given time, and not strictly time-dependent. If a system continues to operate without any change in demand or supply or network configuration, the values of resiliency indices determined will not change over time; however, as the operating conditions vary according to days and seasons, the values of the indices also change correspondingly.

It is important to start the resiliency determination process by determining the number of CLs and sources available in the network, as well as to find the operationally FN solutions to supply power to all CLs during planning and operational contingency. Paths containing more than one CL and/or more than one source are eliminated. By selecting one path for each CL, all possible path combinations to provide power supply to all CLs are listed. To maintain the radial nature of the PDS, path combinations with loop are eliminated using loop elimination technique [32]. Each path combination without loop gives different PN configurations resulting in *unique* networks after eliminating similar networks based on switch configurations. For example, in the multiple-microgrid PDS, switch configurations (both Sectionalizing Switches (all closed) and Tie-line Switches (all open)) of N1, N4, N9 and N12 are same therefore these four networks are reduced to unique network N1. Unique networks satisfying the power flow convergence (using backward-forward sweep technique

TABLE I
DG AND LOAD DATA

Source	Node	Capacity (kVA)		Microgrid
DG1	8	262		1
DG2	16	262		2
Priority	Load Node	P (kW)	Q (kVAR)	Microgrid
Normal	5	48.8	36.6	1
Critical	7	84.5	64.5	
Normal	9	77.3	58.9	
Normal	11	79.9	59.9	
Normal	15	46.6	34.5	2
Normal	17	52.5	39.4	
Critical	19	81.1	60.8	
Normal	21	69.8	52.3	

for unbalanced distribution systems) become FNs satisfying all operating constraints.

Using resiliency quantification process discussed in previous section, network resiliency of each FN is calculated. All FN configurations supplying all CLs are listed in hierarchical order of their resiliency matrices as output of this algorithm.

PCWL gives different PN configurations that gives *unique* networks after eliminating similar networks based on switch configurations. Unique networks satisfying the power flow convergence (using backward-forward sweep technique for unbalanced distribution systems [36]) become FNs satisfying all operating constraints. The forward-backward sweep method is designed to solve the differential algebraic system generated by the maximum principle that characterizes the solution. It is easy to program and runs quickly. Using resiliency quantification process, network resiliency of each FN is calculated and finally compared to get the most resilient network configuration. The DGs are modeled as PV buses and assumed to be capable of meeting the active and reactive power demands of all normal and critical loads of the given network. For each FN capable of feeding all CLs, seven factors affecting the resiliency of the network are considered and the network resiliency is quantified using CI.

Distribution network planner may use this information to find the location and number of sectionalizing and tie-line switches taking into account cost and other related factors. Distribution network operator may take appropriate control actions to enable higher resiliency in power distribution system during contingency based on hierarchical order of resiliency matrices.

V. SIMULATION RESULTS

The proposed algorithm to compute resiliency has been validated using two proximal located CERTS microgrids [37]. The line data and bus data has been obtained from [38]. The DGs and load data are listed in Table I.

The DGs has been located at nodes 8 and 16, capable of serving 165.6 kW critical load demand of the network. The remaining capacity of the generators are used to feed remainder of the normal loads in the same feeder as critical loads. The critical loads CL_1 and CL_2 are identified at nodes 7 and 19, as shown in Fig. 3. There are six normally closed sectionalizing switches and it is possible to install three tie-lines with normally open switches (T_1, T_2 and T_3) in network between nodes 7-11, 17-21, and 11-21.

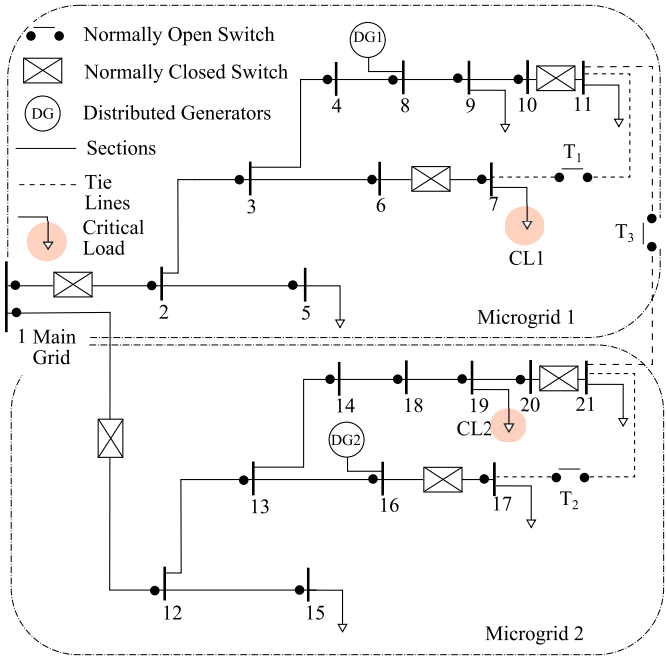

Fig. 3. Test System: Two proximal CERTS Microgrids.

The proposed algorithm may be used to calculate the network resiliency for all FN configurations supplying all CLs in a network that is useful in planning as well as operational stage of a PDS. The application is demonstrated through several case studies. Common objectives for the planning task in general include minimization of losses and cost and maximization of reliability and resiliency. This leads to find the optimal location and size of distributed generation, optimal location and number of reconfigurable switches, etc. Several cases based on possible combinations of tie-line switches are illustrated for planning of resilient network by placing additional switches in a multiple microgrid network. Multiple case studies are also included based on different contingencies during operation. DNO will have the list of FN solutions to be operational and their hierarchy order of resiliency metrics that help the DNO to quickly choose the most resilient network configuration.

In the first step, all the paths are determined using depth-first search algorithm [30]. It is observable that some of the PNs are similar based on switch configurations, so they are reduced to 9 *unique* networks listed in Table II with all sectionalizing and tie-line switches status. In case the critical load is being supplied from the main grid, PoA & PF is considered 0.98 and 0.9 respectively. PoA of each DG is assumed same as 0.95. PF is assumed to be 1, if both DG and CL are in same MG, and PF is assumed to be 0.8, if DG and CL are in different MGs. All nine unique networks are operationally feasible with ± 0.05 pu bus voltage violation limit, therefore the network metrics are quantified for all the nine FNs and listed in Table III. Detailed computation of network metrics for FN1 is shown in the Appendix. For the sake of demonstration of infeasible network paths, the network selection criteria has been made more stringent. Only the first seven unique networks show power flow convergence with ± 0.04 pu bus

TABLE II
UNIQUE NETWORK CONFIGURATIONS WITH CORRESPONDING SIMILAR PNS AND SWITCH CONFIGURATIONS

Unique Network Configurations	Similar PNs	Sectionalizing Switches (NC) 2-1	12-1	7-6	11-10	16-17	20-21	Tie-line Switches (NO) 11-7	21-11	21-17
N_1	N_1, N_4, N_9, N_{12}	C	C	C	C	C	C	O	O	O
N_2	N_2, N_{10}	C	O	C	C	C	C	O	C	O
N_3	N_3, N_{11}	O	C	C	C	C	C	O	C	O
N_4	N_5, N_8	C	C	O	C	C	C	C	O	O
N_5	N_6	C	O	O	C	C	C	C	C	O
N_6	N_7	O	C	O	C	C	C	C	C	O
N_7	N_{13}, N_{16}, N_{18}	C	O	O	C	C	O	C	C	C
N_8	N_{14}, N_{17}, N_{19}	O	C	O	C	C	O	C	C	C
N_9	N_{15}	O	O	O	C	C	O	C	C	C

TABLE III
NETWORK METRICS FOR FEASIBLE NETWORKS (FNS)

	FN1	FN2	FN3	FN4	FN5	FN6	FN7	FN8	FN9
BCE	4.25	5	5	4.25	5	5	4.5	4.5	5
OB	0	0	0	0	3	3	0	0	0
SO	0	2	2	2	4	4	6	6	7
RoS	0.88	0.75	0.75	1	0.50	0.50	0.83	0.83	1
PR	3	3	1.5	3	3	3	3	3	2
PoA & PF	0.84	0.70	0.70	0.81	0.72	0.72	0.66	0.66	0.58
ACPD	0.55	0.62	0.62	0.58	0.62	0.62	0.61	0.60	0.58

TABLE IV
PAIRWISE COMPARATIVE WEIGHTS

	BCE	OB	SO	RoS	PR	PoA & PF	ACPD	Weights
BCE	1	1	3	1	0.33	0.2	0.16	5.64×10^{-2}
OB	1	1	3	1	0.33	0.2	0.16	5.64×10^{-2}
SO	0.33	0.33	1	0.33	0.25	0.16	0.14	2.95×10^{-2}
RoS	1	1	3	1	0.33	0.2	0.16	5.64×10^{-2}
PR	3	3	4	3	1	0.33	0.16	1.21×10^{-1}
PoA & PF	5	5	6	5	3	1	0.25	2.33×10^{-1}
ACPD	6	6	7	6	6	4	1	4.47×10^{-1}

voltage violation limit. The set of FNs is subset of unique networks depending upon operating constraints. The pairwise comparative weights assigned to these network metrics are shown in Table IV.

Table V shows an application of the developed algorithm for planning and designing distribution systems. The table clearly lays out different operational switching states required to supply power to critical loads, and the restoration choices available to an operator for the proximal multiple microgrid system under study, from which the most resilient path must be chosen. Table VI shows the application of the developed algorithm during an ongoing contingency. The CI values, after aggregating impact of all the different criteria for all the 9 FNs using network metrics input values and pairwise comparative weights, are shown in Table VII for three different interaction index values (-0.5, 0 & 1). $\lambda-$measure values are not shown here due to space limitation. The interaction degrees are identified by the importance ratio between maximum input value and minimum input value of network metrics. First, one has to select which input value is important. If one select minimum input value, it means super additive measure is selected. If one select maximum input value, it means sub additive measure is selected. Second, one has to select how much times one put importance. The value is bigger; the output is closer to maximum or minimum input. In this study, even with varying degree of interaction index (-0.5, 0 & 1), the order of PNs in ascending order of their resiliency values remain same, i.e., $FN3$, $FN1$, $FN4$, $FN9$, $FN2$, $FN8$, $FN7$, $FN6$, $FN5$. It implies that relative importance of maximum and minimum values of network metrics are adequately represented in pairwise comparative weights. Broadly PDS planning and operation scenarios are considered for simulation case studies in this paper. Two geographically proximal CERTS microgrids are considered with given DGs, CLs, Tie-lines and sectionalizing switches. Four different operational contingency cases are studied to find the most resilient network configuration.

A. Distribution Planning Scenario

The distribution planning scenario is to be used to develop insights about the resiliency of a system prior to infrastructural investment and development. Drafts of different network designs, load assignments, and DER installation can be evaluated to proactively determine the PDS configuration to be most resilient to physical attacks. In the system being studied in this paper, three tie-line switches between node 7 & node 11 (T_1), between node 17 and node 21 (T_2), and between node 21 and node 11 (T_3) are planned in the network with all possible combinations. Total seven cases corresponding to all possible combinations of three tie-line switches are listed in Table VI. For each combination, all FN configurations supplying all CLs are listed along with their hierarchy order of resiliency metrics. FN with all closed (C) switches (T_1 and/or T_2 and/or T_3) and highest resiliency is considered for planning decision. Three cases (II, IV and VI) are not providing any PN because T_2 switch (alone or with T_1 or T_3 switch) create loop formation therefore made open (O) in FN configuration. N_1 is the only FN without any tie-line switch and has less resiliency compared to all other networks possible in planning decision. This information will help the planners to choose the location and number of additional switches after appropriate trade-off with cost and other factors.

TABLE V
DISTRIBUTION NETWORK PLANNING SCENARIO RESULTS

Cases	Possible Combinations of Tie-line Switches	Feasible Networks (FN) with Tie-line Switch Status				FN in ascending order of Resiliency	Planner Decision
			T_1	T_2	T_3		
I	T_1 Only	$FN1$	O	-	-	$FN4$	$FN4$
		$FN4$	C	-	-		
II	T_2 Only	$FN1$	-	O	-	-	-
III	T_3 Only	$FN1$	-	-	O	$FN3$,$FN2$	$FN2$
		$FN2$	-	-	C		
		$FN3$	-	-	C		
IV	Both T_1 and T_2	$FN1$	O	O	-	-	-
		$FN4$	C	O	-		
V	Both T_1 and T_3	$FN1$	O	-	O	$FN7, FN6$	$FN6$
		$FN2$	O	-	C		
		$FN3$	O	-	C		
		$FN4$	C	-	O		
		$FN6$	C	-	C		
		$FN7$	C	-	C		
VI	Both T_2 and T_3	$FN1$	-	O	O	-	-
		$FN2$	-	O	C		
		$FN3$	-	O	C		
VII	All T_1, T_2, T_3	$FN7$	C	C	C	$FN9$,$FN8$,& $FN7$	$FN7$
		$FN8$	C	C	C		
		$FN9$	C	C	C		

TABLE VI
OPERATIONAL CONTINGENCY SCENARIO RESULTS

Cases	Faulted Nodes	Feasible Networks (FN)	FN in Ascending order of Resiliency	Decision
1	2	$FN1$, $FN2$, $FN3$, $FN4$, $FN5$, $FN6$, $FN7$, $FN8$, $FN9$	$FN3$, $FN1$, $FN4$, $FN2$, $FN9$, $FN8$, $FN7$, $FN6$, $FN5$	$FN5$
2	12	$FN1$, $FN2$, $FN3$, $FN4$, $FN5$, $FN6$, $FN7$, $FN8$, $FN9$	$FN3$, $FN1$, $FN4$, $FN2$, $FN9$, $FN8$, $FN7$, $FN6$, $FN5$	$FN5$
3.A	2,12,11	$FN1$	$FN1$	$FN1$
3.B	2,12,21	$FN1$, $FN4$	$FN1$, $FN4$	$FN4$
4	Sections 3-8, 13-19, 7-11	$FN2$, $FN3$	$FN3$, $FN2$	$FN2$

B. Operational Contingency Scenario

Operational scenarios are important to demonstrate the usability of the proposed metrics to improve distribution network automation, and reduce the chances for power interruption to critical loads. The metric can be used as a future control signal to influence control actions that enable higher resiliency in PDS. Four different contingency cases have been formulated in the multiple CERTS microgrid studied in this paper. They are reported in this section to list all PN configurations supplying all CLs along with their hierarchy order of resiliency metrics (listed for each case in Table VII).

Case 1: In this case, it is assumed that a fault occurred at one of main grid's feeder to MG-1. Fault at node 2 will island the MG-1 from main grid and will result in exclusion of all PCWL passing through node 2. Out of 19 PNs, four networks (*FN*1, *FN*2, *FN*3, *FN*4) will not be operational. Due to similarity overlapping of PNs all nine FN solutions will still be operational for supplying all CLs. DNO should choose the network with highest resiliency, i.e., *FN*5, where CL1 and CL2 are both supplied by DG1.

If the most resilient topology is infeasible, the proposed algorithm selects the next feasible most resilient topology. In Case I under Distribution Planning Scenario, *FN*1 is the only FN without any tie-line switch and has less resiliency compared to all other networks possible in planning decision. In this case, only *FN*1 can be adopted and will be the most resilient feasible topology adopted for the system.

TABLE VII
CHOQUET INTEGRAL VALUES WITH VARYING INTERACTION DEGREE

Feasible Networks (FN)	Choquet Integral With λ= -0.5	λ=0	λ=1
$FN1$	123.3	109.3	95.2
$FN2$	133.2	118.9	104.7
$FN3$	111.2	100.7	90.2
$FN4$	130.1	116.5	102.8
$FN5$	156.3	140.9	125.5
$FN6$	156.1	140.6	125.2
$FN7$	142.5	126.5	110.6
$FN8$	141.9	125.8	109.9
$FN9$	133.2	118.0	102.9

Case 2: In this case, it is assumed that a fault occurred at one of main grid's feeder to MG-2. Fault at node 12 will island the MG-2 from main grid and will result in elimination of all PCWL passing through node 12. Out of 19 PNs, five networks (N_1, N_5, N_9, N_{13}, N_{14}) will not be operational. Due to similarity overlapping of PNs all nine FN solutions will still be operational for supplying all CLs. DNO should choose the network with highest resiliency, i.e., *FN*5.

Case 3: In this case, it is assumed that microgrids MG-1 and MG-2 both are in islanded mode due to fault in their

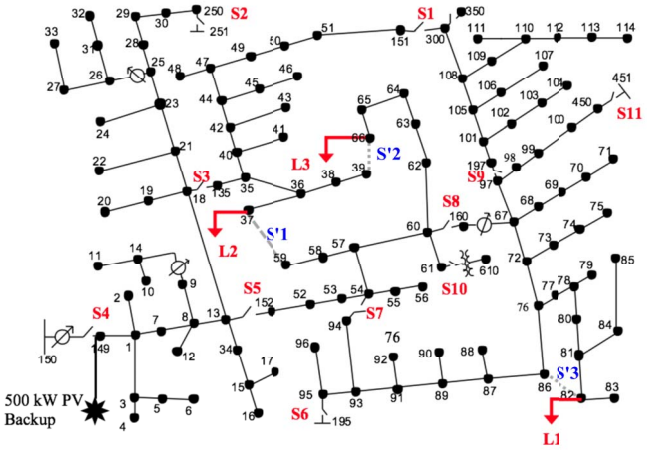

Fig. 4. Modifications made to standard IEEE 123 node distribution system.

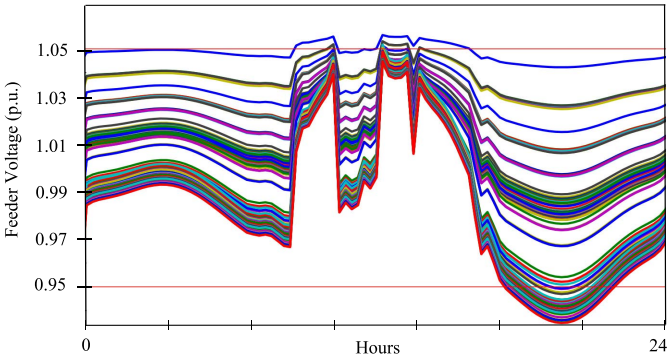

Fig. 5. Voltage profiles of all nodes over a 24 hour load-profile.

feeder to main grid and also fault in tie line between MG-1 and MG-2. This case is realized with two different scenarios. Scenario 1 is considered with fault at nodes 2, 12 and 11. This will reject all PCWL passing through these three nodes and only one PN (N_{12}) will be operational. Therefore, the DNO will not have any choice and has to operate corresponding FN, i.e., *FN*1. In scenario 2, fault at nodes 2, 12 and 21 may be considered to realize the same case. This will reject all PCWL passing through nodes 2, 12 and 21 and only two PNs (N_8, N_{12}) will be operational. Thus the DNO will have a choice between corresponding FNs (*FN*1, *FN*4) and will chose the network with higher resiliency, i.e., *FN*4.

Case 4: In this case, it is assumed that both the MGs are grid connected and their interconnected tie line is also healthy but the fault happens within MGs due to a storm hitting several areas, such that the lines between Bus-3 to Bus-8, lines between Bus 13 to Bus 19 and line between Bus 7 to Bus 11 are out of service. This will result in elimination of all PCWL passing through paths joining these nodes. Out of 19 PNs, only two networks (N_2, N_3) will be operational. This leads to corresponding two FN solutions (*FN*2, *FN*3) to be operational for supplying all CLs. Therefore, the DNO will chose the network with higher resiliency, i.e., *FN*2.

C. Application to IEEE 123 Node Distribution System

In order to demonstrate the scalability of the proposed approach for implementation in a operational setting of a larger system, IEEE 123 node PDS has been chosen for demonstration. IEEE 123 node PDS is an unbalanced and multi-phase radial distribution network with 11 three phase switches [39]. There are enough switches in the feeder so that multiple paths for restoring a load can be tested, and resiliency metric for each corresponding path can be easily determined. Some assumptions have been made in this paper for the IEEE 123-bus test system:

1) Assumed all loads are modeled as constant PQ loads.
2) Three critical loads have been assumed to be at Node 66 (single phase load *Load 1* - 75 kW and 35 kVAr), Node 37 (single phase load *Load 2*- 40 kW and 20 kVAr) and Node 82 (single phase load *Load 3*- 40 kW and 20 kVAr), as shown in Fig. 4
3) Three sectionalizing switches S'1, S'2 and S'3 were installed between nodes 37 and 59, 39 and 66 and 82 and 86, respectively, as shown in Fig. 4
4) DNO has control limited to the three phase switches and the added sectionalizng switches
5) 500 kW renewable generation (with storage) has been modeled at node 149 in order to supply power in the system in event of failures upstream of the substation (node 150).

The total load of the system is 1420 kW, and scaled to fit a load profile from PJM's 2010 metered historical data [40]. Therefore, the load profile of the 123 node distribution system is normalized so that its peak value is 1 and multiplied by the value of the static load at each bus.

Due to the integration of a 500 kW solar backup power system in the PDS, the voltage profiles at several nodes go beyond the 1.0 ± 0.05 p.u. operational limits, as shown in Fig. 5. The number of paths available to restore Load 1, Load 2, and Load 3 have varying number of paths available for restoration, depending on time of day (as shown in Fig. 6). Since, the resiliency of network is dependent on the number of paths available for restoration, it may be concluded from this simulation that resiliency of the network is a function of the operational state, and the operator needs to be informed in real-time about the most resilient path for restoring a critical load, with respect to the ongoing system conditions.

In Fig. 6, all possible paths for restoring the loads, for all PNs has been computed.

Let us consider a scenario where the PDS is islanded from the grid and being sustained on the 500 kW solar generation backup at 10 AM on the day of the chosen load profile. Also, uncleared faults are being repaired by crews in the sections 35 and 36, 63 and 64, and 72 and 76 - such that the DNO is tasked with restoring all critical loads (Load 1, Load 2, and Load 3) in the most resilient configuration, before normal operation can be resumed. In this scenario, the proposed approach of the paper, will present the DNO with the switching actions that can be executed in the system and corresponding resiliency value for the path to restore the load. The ranking of switching actions is shown in Table VIII. For brevity (and clarity of understanding of the DNO), only the top three resilient

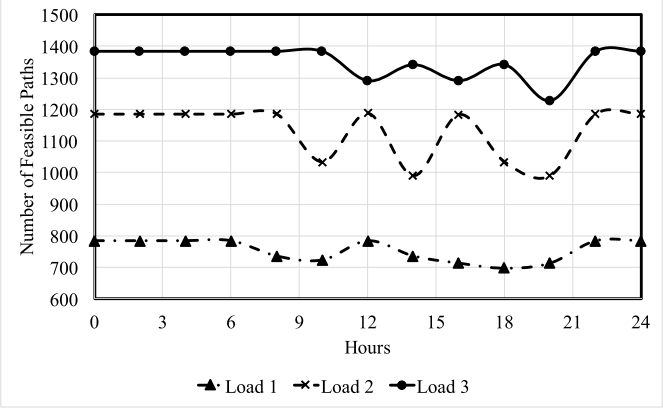

Fig. 6. Diurnal variation of number of available paths for load restoration.

TABLE VIII
RESILIENCY METRIC RANKING TABLE FOR CRITICAL LOAD RESTORATION

Net-work	Switching Operation (O: Open, C: Close)	CI Resiliency Metrics Load 1	Load 2	Load 3
$FN1$	O:S3, S'1 C: S4, S'2, S5, S8	134.2	127.9	164.2
$FN2$	O:S5, C:S'1, S'2, S8	133.3	167.9	147.3
$FN3$	O:S5, S8, S'2 C: S7, S'1	131.2	148.9	154.2

configuration options are presented in the table, though the preference can be customized. The resiliency values are computed using Eqs. (8)-(11), with an interaction value of $\lambda = 0$, implying the factors affecting resiliency impact the overall resiliency value independently, without any positive or negative synergy. The ranking table is sorted according to the most resilient configuration for Load 1, but can be re-arranged according to the preference of the DNO. The impact of the switching actions to the paths restoring Load 2 and Load 3 are also presented. In this way, the operator's decision making for the switching operation can be aided during contingencies.

From Table VIII, it can be interpreted that $FN1$ is is the most resilient path to provide power to Load 1 and Load 3, while $FN2$ is the most resilient path to provide power to Load 2.

1) Meshed or Ring Main Distribution Topology: Though PDS in North America and worldwide are predominantly radial in nature, the proposed algorithm is valid for meshed distribution systems as well. Meshed (or Ring Main) distribution topology is characterized by greater feeder redundancy and loop formation in the network. By taking out the radial constraints imposed in the proposed approach, such as loop elimination, the algorithm shown in Fig. 2 will work for meshed or ring networks. A meshed network is characterized by presence of loops formed by strategically placed switches in the PDS. Loops in a meshed network are achieved by making tie-line switches status as normally closed (NC) instead of being normally open (NO) as in radial distribution feeders. In the multiple CERTS microgrid system case study shown in Fig. 3, switches T_1, T_2 and T_3 would be NC for meshed topology. As a result, the only unique network configurations feasible would be restricted to $N_7, N_8, N_9, N_{13}, N_{14}, N_{15}, N_{16}, N_{17}, N_{18}$ and N_{19}, as shown in Table II. The rest of the computation of network metrics (as in Table III) and subsequent derivation of the resilient metrics of the FNs is identical for both radial and meshed distribution topologies. Results have not be shown here to avoid redundancy in results. Thus, the approach is suitable for both radial and meshed distribution topologies.

2) Computation Costs: In order to check the feasibility of the proposed solution to real-world distribution systems, the computation cost for generating the resiliency value ranking table was also considered. The memory requirement for computation of all feasible configurations based on a network positively depends upon the number of nodes in the network. Each node accounted for 19 bytes of memory while running the 123-node PDS simulation, and required 17.83 kilobytes of random-access memory (RAM) for processing. For larger networks, the memory requirement is a function of $\mathcal{O}(2^s.ne + \log n)$, where n is the number of nodes and e is the number of branches in the PDS [28]. Thus, it can be estimated for a typical distribution with 10,000 nodes, the memory requirement is 26.12 megabytes of RAM - which is well within a capacity of single-threaded modern digital computers installed in distribution automation control centers. The processing power is further enhanced if multiple threads of the computer are used, but that was not explored in this work.

VI. CONCLUSION

A novel problem formulation and solution approach for measuring and enabling resiliency of a PDS has been presented in this paper. The algorithm proposed in this paper can be used by DNOs to determine the most resilient paths to restore critical loads, under all possible contingencies feasible in the network. An array of all feasible paths corresponding to any loss-of-source situation is ranked, and available to the distribution system operator. The paths are determined optimally to maximize the resiliency of the power distribution system. The simulations validate the conjecture that resiliency of a network depends on number of paths to connect a source node to a sink node, and ratio of number of sources to number of critical load. The simulation results also show that increasing number of number of switches increases resiliency, but increasing number of switching operations decrease the resiliency - as more switches means more points of failures.

The Choquet Integral approach is not computationally expensive, and can be applied to large batches of feasible paths to restore a load. Moreover, distribution planner may use this information to find the number and locations of switches to enable higher resiliency in power distribution network.

The proposed algorithm has been validated using a model of two geographically proximal industry standard CERTS microgrids for all PNs configurations. The approach has been further validated using IEEE 123 node distribution feeder. This paper also illustrates the application of the proposed algorithm in distribution network planning as well as in the operational contingency scenarios. The solution approach will be extended in future by including duration of time taken to restore service to CLs following a power outage. Similarly in planning scenario, placement of DGs and additional lines needed to improve resiliency will be considered in a future work.

TABLE IX
PCWL CORRESPONDING TO 4 PNS

PNs	Path 1 for CL1	Path 2 for CL2
N_1	7,6,3,2,1	19,18, 14,13,12,1
N_2	7,6,3,2,1	19,18,14,13,16
N_3	7,6,3,4,8	19,18, 14,13,12,1
N_4	7,6,3,4,8	19,18,14,13,16

TABLE X
POA & PF FOR EACH PN

PNs	Sources for CL1			Sources for CL2		
	PoA	PF	PoA X PF	PoA	PF	PoA X PF
N_1	0.98	0.9	0.882	0.98	0.9	0.882
N_2	0.98	0.9	0.882	0.95	1	0.95
N_3	0.95	1	0.95	0.98	0.9	0.882
N_4	0.95	1	0.95	0.95	1	0.95

TABLE XI
COMPUTATION OF *ACPD* FOR *FN*1

Node(d)	OrderΩ	$C_B(d)$	$\Omega \times C_B(d)$
1	2.00	0.179	0.357894737
2	3.00	0.274	0.821052632
3	3.00	0.316	0.947368421
4	2.00	0.289	0.578947368
5	2.00	0.205	0.410526316
6	1.00	0.000	0
7	2.00	0.100	0.2
8	2.00	0.189	0.378947368
9	2.00	0.333	0.666315789
10	2.00	0.263	0.526315789
11	1.00	0.000	0
12	2.00	0.268	0.536842105
13	3.00	0.584	1.752631579
14	3.00	0.568	1.705263158
15	3.00	0.582	1.744736842
16	2.00	0.153	0.305263158
17	2.00	0.137	0.273684211
18	2.00	0.147	0.294736842
19	1.00	0.000	0
20	1.00	0.000	0
21	1.00	0.000	0
ACPD($FN1$)			**11.5005/21 = 0.55**

APPENDIX
NETWORK METRICS COMPUTATION EXAMPLE

Network metrics for all the nine FNs are listed in Table III. Detailed calculation of all network metrics values only for *FN*1 is shown here. There are 4 similar PNs (N_1, N_4, N_9, N_{12}) for FN1 as their switch configurations (shown in Table II) are same. So q is equal to 1; and N_q is equal to 4 for *FN*1. Sequence of nodes for the PCWL, corresponding to these 4 PNs is listed in Table IX.

- Nodes in PCWL for $N1, N4, N9, N12$ are 9, 8, 9 and 8 respectively and number of CLs is same (i.e., 2) for all. So $BCE_1 = ((9/2 + 8/2 + 9/2 + 8/2))/4 = 4.25$
- Number of common branches in each PN ($N1, N4, N9, N12$) is zero. So $OB_1 = 0$.
- As shown in Table II, all Sectionalizing Switches are closed and all Tie-line Switches are open for all PNs ($N1, N4, N9, N12$). So there is no change in switch configuration from normal position, therefore, $SO_1 = 0$.
- Number of sources supplying all CLs in PNs ($N1, N4, N9, N12$) are 1, 2, 2 and 2 respectively and number of CLs for all PNs is 2. So $ROS_1 = ((1/2 + 2/2 + 2/2 + 2/2))/4 = 0.875$.
- Each CL has 3 paths available to connect to all 3 sources in *FN*1. So $PR_1 = ((3 + 3))/2 = 3$.
- Calculation for PoA & PF for each PN is listed in Table X based on values given in Section V. PoA & PF $= ((0.882 \times 0.882) + (0.882 \times 0.95) + (0.882 \times 0.95) + (0.95 \times 0.95))/4 = 0.8391 \sim 0.84$.
- $ACPD_1$ depends on order and CB of each node in *FN*1. For *FN*1, $D = 21$. Order of each node, and corresponding betweenness centrality of each node d (i.e., $C_B(d)$) are shown in Table XI. Betweenness Centrality of each node is computed from Eq. 6, using MATLAB's graph analysis libraries. Exactly similar results can be obtained by creating an undirected graph of the multiple microgrid distribution system using any network analyzing software, such as Cytoscape [41].

REFERENCES

[1] C. Marnay *et al.*, "Japan's pivot to resilience: How two microgrids fared after the 2011 earthquake," *IEEE Power Energy Mag.*, vol. 13, no. 3, pp. 44–57, May/Jun. 2015.

[2] Z. Wang, B. Chen, J. Wang, and C. Chen, "Networked microgrids for self-healing power systems," *IEEE Trans. Smart Grid*, vol. 7, no. 1, pp. 310–319, Jan. 2016.

[3] S. Bahramirad, A. Khodaei, J. Svachula, and J. R. Aguero, "Building resilient integrated grids: One neighborhood at a time," *IEEE Electrification Mag.*, vol. 3, no. 1, pp. 48–55, Mar. 2015.

[4] L. Che, X. Zhang, and M. Shahidehpour, "Resilience enhancement with DC microgrids," in *Proc. IEEE Power Energy Soc. Gen. Meeting*, Denver, CO, USA, 2015, pp. 1–5.

[5] Z. Wang and J. Wang, "Self-healing resilient distribution systems based on sectionalization into microgrids," *IEEE Trans. Power Syst.*, vol. 30, no. 6, pp. 3139–3149, Nov. 2015.

[6] E. D. Vugrin, D. E. Warren, and M. A. Ehlen, "A resilience assessment framework for infrastructure and economic systems: Quantitative and qualitative resilience analysis of petrochemical supply chains to a hurricane," *Process Safety Progr.*, vol. 30, no. 3, pp. 280–290, 2011.

[7] Office of the press in The White House, "Critical infrastructure security and resilience," United States Presidential Policy Directive-21, Feb. 2013, accessed on Nov. 2016. [Online]. Available: https://www.whitehouse.gov/the-press-office/2013/02/12/presidential-policy-directive-critical-infrastructure-security-and-resil

[8] J.-P. Watson *et al.*, "Conceptual framework for developing resilience metrics for the electricity, oil, and gas sectors in the United States," Sandia Nat. Lab., Albuquerque, NM, USA, Tech. Rep. SAND2014-18019, Sep. 2015.

[9] F. D. Petit *et al.*, "Resilience measurement index: An indicator of critical infrastructure resilience," Dept. Decis. Inf. Sci. Div., Argonne Nat. Lab., Lemont, IL, USA, Tech. Rep. ANL/DIS-13-01, 2013.

[10] S. D. Manshadi and M. E. Khodayar, "Expansion of autonomous microgrids in active distribution networks," *IEEE Trans. Smart Grid*, Aug. 2016, doi: 10.1109/TSG.2016.2601448.

[11] H. Gao, Y. Chen, Y. Xu, and C.-C. Liu, "Resilience-oriented critical load restoration using microgrids in distribution systems," *IEEE Trans. Smart Grid*, vol. 7, no. 6, pp. 2837–2848, Nov. 2016.

[12] R. Arghandeh, A. von Meier, L. Mehrmanesh, and L. Mili, "On the definition of cyber-physical resilience in power systems," *Renew. Sustain. Energy Rev.*, vol. 58, pp. 1060–1069, May 2016.

[13] A. Kwasinski, "Quantitative model and metrics of electrical grids' resilience evaluated at a power distribution level," *Energies*, vol. 9, no. 2, p. 93, 2016.

[14] Y. Xu, C.-C. Liu, K. P. Schneider, and D. T. Ton, "Toward a resilient distribution system," in *Proc. IEEE Power Energy Soc. Gen. Meeting*, Denver, CO, USA, 2015, pp. 1–5.

[15] A. Khodaei, "Resiliency-oriented microgrid optimal scheduling," *IEEE Trans. Smart Grid*, vol. 5, no. 4, pp. 1584–1591, Jul. 2014.

[16] R. Albert and A.-L. Barabási, "Statistical mechanics of complex networks," *Rev. Mod. Phys.*, vol. 74, no. 1, p. 47, 2002.
[17] X. F. Wang and G. Chen, "Complex networks: Small-world, scale-free and beyond," *IEEE Circuits Syst. Mag.*, vol. 3, no. 1, pp. 6–20, Sep. 2003.
[18] A. Pandit, H. Jeong, J. C. Crittenden, and M. Xu, "An infrastructure ecology approach for urban infrastructure sustainability and resiliency," in *Proc. IEEE/PES Power Syst. Conf. Expo. (PSCE)*, Phoenix, AZ, USA, 2011, pp. 1–2.
[19] D. T. Nguyen, Y. Shen, and M. T. Thai, "Detecting critical nodes in interdependent power networks for vulnerability assessment," *IEEE Trans. Smart Grid*, vol. 4, no. 1, pp. 151–159, Mar. 2013.
[20] S. Chanda and A. K. Srivastava, "Defining and enabling resiliency of electric distribution systems with multiple microgrids," *IEEE Trans. Smart Grid*, vol. 7, no. 6, pp. 2859–2868, Nov. 2016.
[21] S. Chanda, "Measuring and enabling resiliency in distribution systems with multiple microgrids," M.S. thesis, School Elect. Eng. Comput. Sci., Washington State Univ., Pullman, WA, USA, 2015.
[22] A. Arab *et al.*, "Stochastic pre-hurricane restoration planning for electric power systems infrastructure," *IEEE Trans. Smart Grid*, vol. 6, no. 2, pp. 1046–1054, Mar. 2015.
[23] S. D. Manshadi and M. E. Khodayar, "Resilient operation of multiple energy carrier microgrids," *IEEE Trans. Smart Grid*, vol. 6, no. 5, pp. 2283–2292, Sep. 2015.
[24] K. Schneider *et al.*, "Evaluating the feasibility to use microgrids as a resiliency resource," *IEEE Trans. Smart Grid*, Mar. 2016, doi: 10.1109/TSG.2015.2494867.
[25] C. Chen, J. Wang, F. Qiu, and D. Zhao, "Resilient distribution system by microgrids formation after natural disasters," *IEEE Trans. Smart Grid*, vol. 7, no. 2, pp. 958–966, Mar. 2016.
[26] Y. Wang, C. Chen, J. Wang, and R. Baldick, "Research on resilience of power systems under natural disasters—A review," *IEEE Trans. Power Syst.*, vol. 31, no. 2, pp. 1604–1613, Mar. 2016.
[27] F. Rubin, "Enumerating all simple paths in a graph," *IEEE Trans. Circuits Syst.*, vol. 25, no. 8, pp. 641–642, Aug. 1978.
[28] D. E. Knuth, "Big omicron and big omega and big theta," *ACM SIGACT News*, vol. 8, no. 2, pp. 18–24, 1976.
[29] P. Mateti and N. Deo, "On algorithms for enumerating all circuits of a graph," *SIAM J. Comput.*, vol. 5, no. 1, pp. 90–99, 1976.
[30] R. Tarjan, "Depth-first search and linear graph algorithms," *SIAM J. Comput.*, vol. 1, no. 2, pp. 146–160, 1972.
[31] J. L. Cochrane and M. Zeleny, *Multiple Criteria Decision Making*. Columbia, SC, USA: Univ. South Carolina Press, 1973.
[32] C. Labreuche and M. Grabisch, "The Choquet integral for the aggregation of interval scales in multicriteria decision making," *Fuzzy Sets Syst.*, vol. 137, no. 1, pp. 11–26, 2003.
[33] E. Takahagi, "λ fuzzy measure identification methods using λ and weights," Dept. School Commerce, Senshu Univ., Tokyo, Japan, Mar. 2005, accessed on Nov. 2016. [Online]. Available: http://www.isc.senshu-u.ac.jp/~thc0456/Efuzzyweb/mant2/fz_sou.pdf
[34] K. Leszczyński, P. Penczek, and W. Grochulski, "Sugeno's fuzzy measure and fuzzy clustering," *Fuzzy Sets Syst.*, vol. 15, no. 2, pp. 147–158, 1985.
[35] R. A. Jabr, "Polyhedral formulations and loop elimination constraints for distribution network expansion planning," *IEEE Trans. Power Syst.*, vol. 28, no. 2, pp. 1888–1897, May 2013.
[36] Z. Wang, F. Chen, and J. Li, "Implementing transformer nodal admittance matrices into backward/forward sweep-based power flow analysis for unbalanced radial distribution systems," *IEEE Trans. Power Syst.*, vol. 19, no. 4, pp. 1831–1836, Nov. 2004.
[37] R. Lasseter *et al.*, "The CERTS microgrid concept," White Paper, Transm. Rel. Program, Office Power Technol., U.S. Dept. Energy, Washington, DC, USA, 2002.
[38] F. A. Martina, "Graph theory and particle swarm based reconfiguration of multiple microgrids for grid resiliency," M.S. thesis, School Elect. Eng. Comput. Sci., Washington State Univ., Pullman, WA, USA, 2014.
[39] W. H. Kersting, "Radial distribution test feeders," in *Proc. IEEE PES Power Eng. Soc. Win. Meeting*, vol. 2. Columbus, OH, USA, 2001, pp. 908–912.
[40] R. Sioshansi, P. Denholm, T. Jenkin, and J. Weiss, "Estimating the value of electricity storage in PJM: Arbitrage and some welfare effects," *Energy Econ.*, vol. 31, no. 2, pp. 269–277, 2009.
[41] P. Shannon *et al.*, "Cytoscape: A software environment for integrated models of biomolecular interaction networks," *Genome res.*, vol. 13, no. 11, pp. 2498–2504, 2003.

Prabodh Bajpai (SM'16) received the Ph.D. degree in electrical engineering from IIT Kanpur, India. He is currently as an Associate Professor with the Department of Electrical Engineering, IIT Kharagpur, India. His research interests include power system restructuring, renewable energy systems, and power system optimization.

Sayonsom Chanda received the master's degree in electrical engineering from Washington State University and works as a Research Engineer with the Power and Energy Department, Idaho National Laboratory. His research interests include reliability and resiliency of power distribution systems, integration of energy systems devices for power grid applications and hardware-in-the-loop simulations. He is registered as an Engineer-in-Training in the state of Idaho, USA.

Anurag K. Srivastava received the Ph.D. degree in electrical engineering from the Illinois Institute of Technology, Chicago, IL, USA, in 2005. He is an Associate Professor of Power Engineering at Washington State University. His research interests include power system operation and control, synchrophasors applications, microgrid resiliency, and cyber-physical analysis of power system. He is an Associate Editor of the IEEE TRANSACTIONS ON SMART GRID and *IET Generation, Transmission and Distribution*. He is an IEEE Distinguished Lecturer.